Color Glass Condensate signatures and phenomenology at RHIC and LHC.

Prithwish Tribedy

Variable Energy Cyclotron Center, Kolkata, India

Sept 10, 2013

Triggering Discoveries in High Energy Physics, Jammu, India

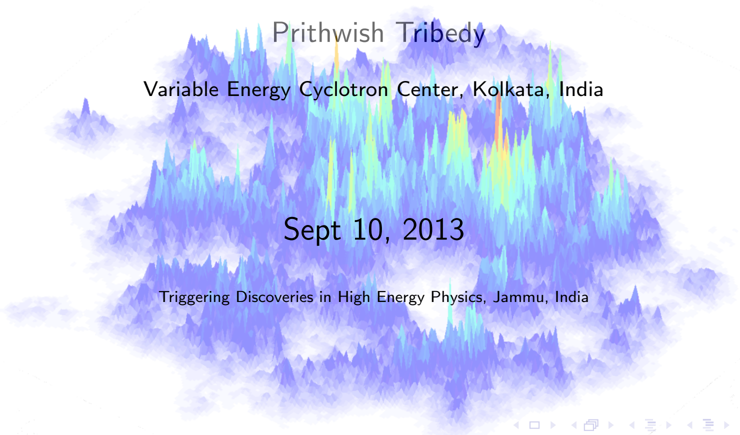

Outline

- Intoduction.
- DIS processes at HERA and Gluon Saturation.
- The Color Glass Condensate & framework of CYM.
- Inclusive multiplicity & multi-particle correlation.
- Modelling initial stage geometry in p+p, p+A and A+A collisions.

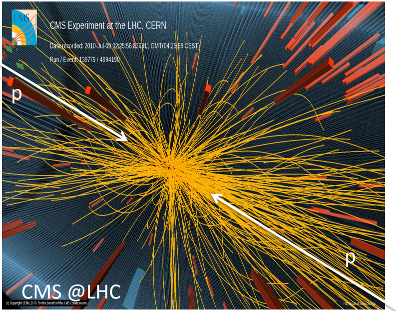

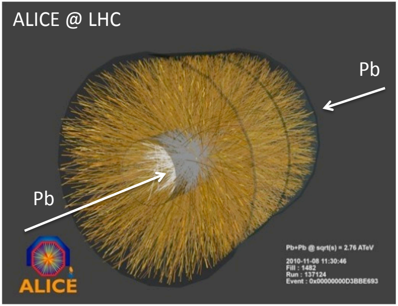

- Why does number of produced particles fluctuate from event-to-event ?
- Can we calculate how many particles are produced in an *ab-initio* approach?

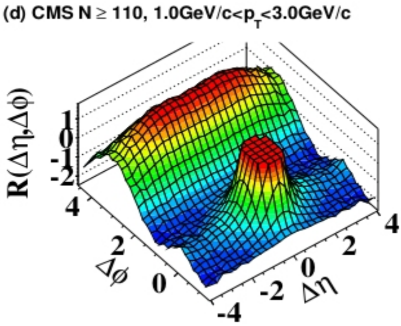

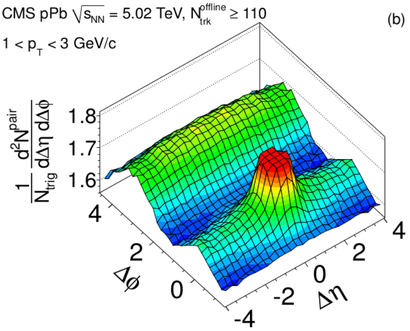

- How does collimation come? What is the source of intrinsic ridge and long range correlation?

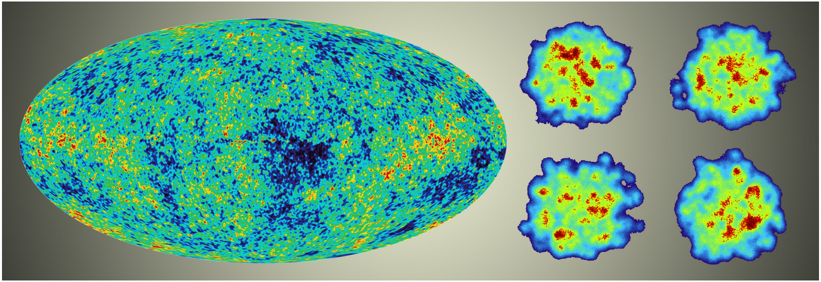

- What is the scale of initial quantum fluctuations in the mini-bang ?

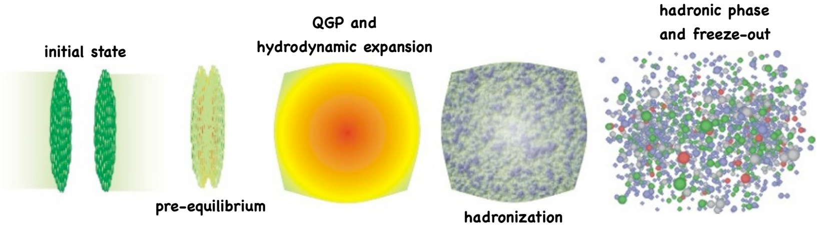

Standard model of heavy ion collisions:

- How to get an *ab initio* description of the early stages of HIC?
- How to constrain the transport coefficients ?

DIS process at HERA

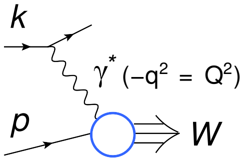

High energy limit → small x limit of QCD

$$(x \approx \frac{Q^2}{E_{cms}^2} = \frac{Q^2}{s})$$

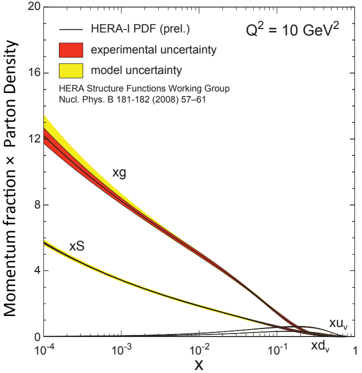

HERA e-p scattering probes protons with :

Transverse resolution $\Delta r_\perp \sim \frac{1}{Q}$

Time resolution $\Delta t \sim \frac{2xp}{Q^2}$

→ Rapid growth of gluons at small x

High energy hadrons/nuclei

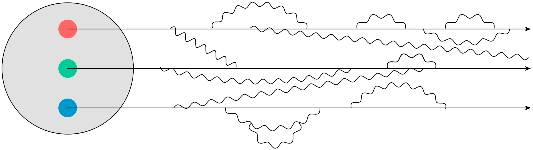

Hadron at rest

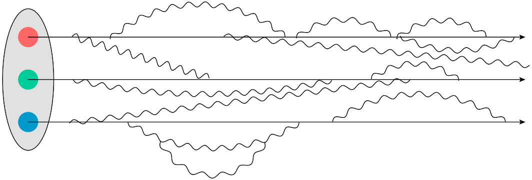

Boosted hadron

At high energies interaction time scales of fluctuations dilated well beyond typical hadronic time scales.

DIS: Snapshot of hadrons/nuclei

$$\Delta r_\perp \sim \frac{1}{Q} \quad , \quad \Delta t \sim \frac{2xp}{Q^2} \quad , \quad x = \frac{Q^2}{s}$$

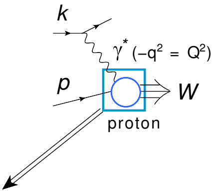

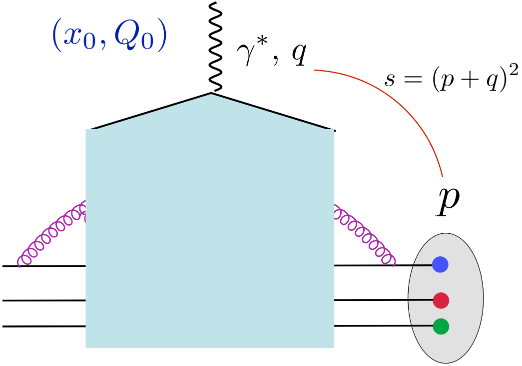

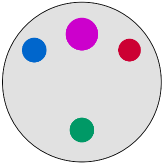

figure: Albacete QM′12

DIS: Snapshot of hadrons/nuclei

$$\Delta r_\perp \sim \frac{1}{Q} \quad , \quad \Delta t \sim \frac{2xp}{Q^2} \quad , \quad x = \frac{Q^2}{s}$$

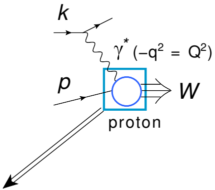

$(x < x_0, Q > Q_0)$

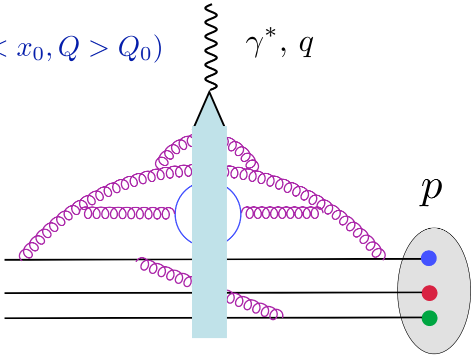

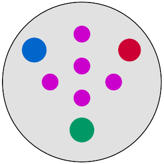

figure: Albacete QM′12

Finer resolution reveals more sub structure (higher Fock states) at smaller x, $|H\rangle = |qqq\rangle + |qqqg\rangle + \cdots + |qqqgg \ldots gg\rangle$

QCD evolution equations

$$dP_{q/g\to g} = \frac{\alpha_s C_F/A}{\pi} \frac{dx}{x} \frac{d^2 k_\perp}{k_\perp^2}$$

BFKL Evolution

Fixed $Q^2, x \to 0$

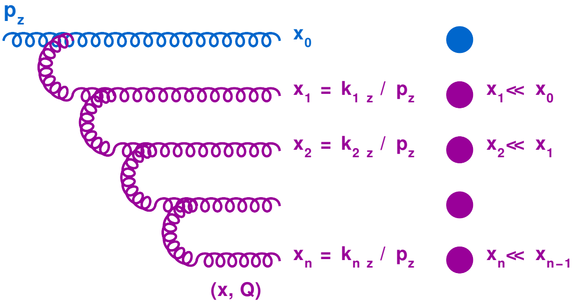

Probability of emitting n gluons $\mathcal{P}(n) \sim \frac{1}{n!}\left(\alpha_s \ln\left(\frac{x_0}{x}\right)\right)^n$

$\rightarrow$ enhanced by large logarithms

QCD evolution equations

BFKL growth is linear

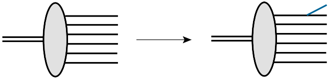

BFKL equation:

PDF $xg(x) \approx \int d^2k_\perp \phi(x, k_\perp)$

$$\frac{\partial \phi(x, k_\perp)}{\partial \log(x_0/x)} \approx \mathcal{K} \otimes \phi(x, k_\perp)$$

$$\to \phi_{\text{BFKL}} \sim x^{\alpha_s}$$

$$\Rightarrow \sigma_{tot}^{p+p} \sim s^{\alpha_P - 1}$$

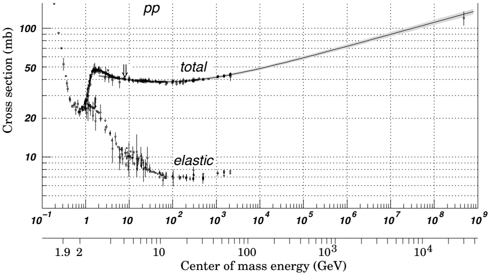

(Experimental σ_{tot} $\to$ grows logarithmically)

Linear Bremstrahlung growth of PDF $\to$ power law growth of cross section

$\to$ Violates black disc limit as $\sigma_{tot} \leq 2\pi R^2$

Froissart - Martin unitarity bound ($\sigma_{tot} \sim \ln^2 s$)

QCD Evolution equations

Non-linear recombination processes constrain the growth
$\rightarrow$ Saturation

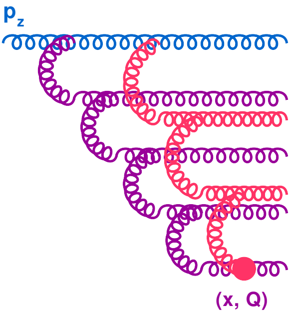

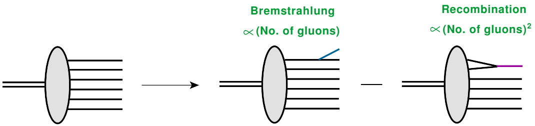

$$\frac{\partial \phi(x, k_\perp)}{\partial \log(x_0/x)} \approx \mathcal{K} \otimes \phi(x, k_\perp) - \phi(x, k_\perp)^2 \quad \textit{BK/JIMWLK equation}$$

Non-linear equation gives rise a scale, $Q_s^2(x) \rightarrow$ saturation scale.

Gluon saturation

Gribov, Levin, Ryskin 1983

No of gluons of a fixed size saturates due to phase space constrain.

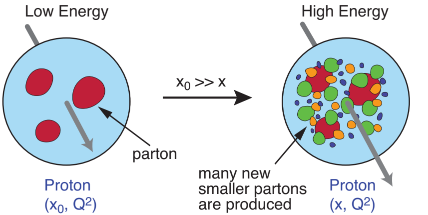

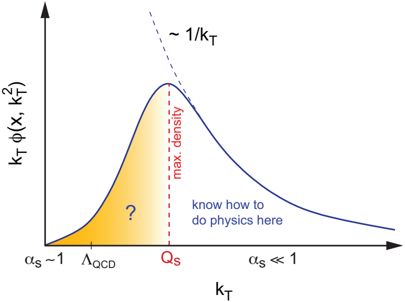

figure: 1212.1701

Density saturates with max. occupancy $\sim \mathcal{O}(\frac{1}{\alpha_s})$ for $k_T \leq Q_S(x)$

Higher energy $\rightarrow$ larger $Q_s \gg \Lambda_{QCD}$, effective coupling $\alpha_S(Q_S)$ is small

Geometric scaling

DIS cross section scales with

$$\tau = \frac{Q^2}{Q_S(x)^2}$$

$$\sigma_{DIS}(x, Q^2) = \sigma_{DIS}\left(Q^2/Q_S^2(x)\right)$$

p+p multiplicity scales with

$$\tau = \frac{p_T^2}{Q_S(x)^2} \text{ or } \frac{p_T}{Q_S}, \left(x \equiv \frac{p_T}{\sqrt{s}} e^{\pm y}\right)$$

$$\frac{1}{\sigma}\frac{dN_{ch}}{d\eta d^2 p_T} = F\left(\frac{p_T}{Q_S(p_T/\sqrt{s})}\right)$$

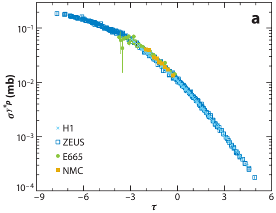

Stasto, Golec-Biernat & Kwiecinski 2001
Levin, Tuchin '99, Iancu, Itakura, McLerran '02

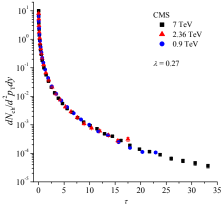

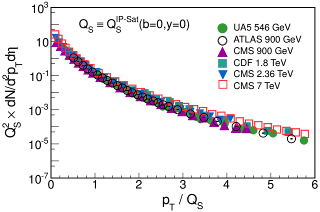

McLerran & Praszalowicz 2010, PT & Venugoapalan 2010

Saturation scale $Q_S(x)$ is the dominant scale controlling the dynamics of particle production in $e + p$ and $p + p$.

Universality and Nuclear oomph

Gluon saturation → Universal phenomenon to hadrons/nuclei.

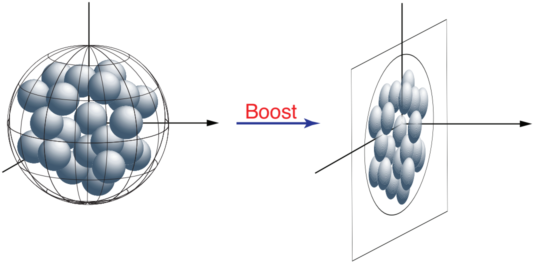

For large nucleus, thickness $R \sim A^{1/3}$,

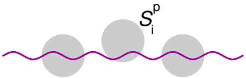

Gluon momentum gets → $A^{1/3}$ transverse momentum random "kicks"

Nuclear Saturation scale $(Q_s^A)^2 \approx A^{1/3}(Q_s^p)^2$ → Nuclear *oomph*

Saturation models of HERA DIS

Bartels, Golec-Biernat, Kowalski
Kowalski, Teaney

How to extract satiation scales/hadronic wave functions from HERA data?

Cross section in $e + p$ collisions is parametrized

The dipole scattering matrix for proton is

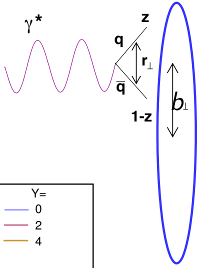

$$S^p_{\rm dip}(\mathbf{r}_\perp, x, \mathbf{b}_\perp) = \exp\left(-r^2 Q_S(x,b)^2\right)$$

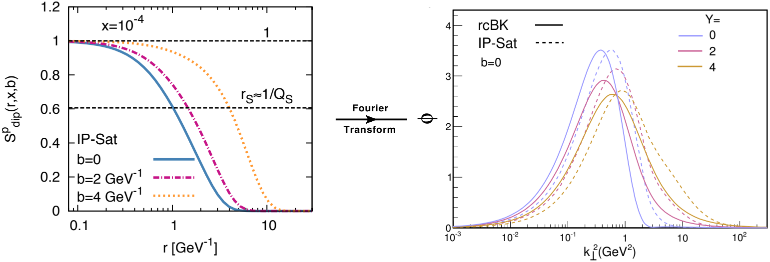

Saturation condition

$$S^p_{\rm dip}(\mathbf{r}_\perp = r_S, x, \mathbf{b}_\perp) = \exp(-1/2) \implies Q_s^2 = \frac{2}{r_S^2}$$

Color charge distribution inside Nuclei

The nuclear scattering matrix is obtained as

$$S^A_{\rm dip}(\mathbf{r}_\perp, x, \mathbf{b}_\perp) = \prod_{i=0}^{A} S^p_{\rm dip}(\mathbf{r}_\perp, x, \mathbf{b}_\perp)$$

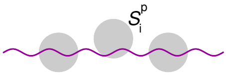

$i \rightarrow$ nucleons are distributed according to Fermi dist

$S^A_{\rm dip} \rightarrow$ distribution of nuclear saturation scale
$\rightarrow$ distribution of color charge density.

Lumpy color charge density distribution $g^2\mu(\mathbf{x}_\perp) \sim Q_s(\mathbf{x}_\perp)$

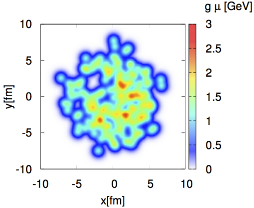

Kowalski, Lappi, Venugopalan 0705.3047
Lappi, arXiv:0711.3039, 1104.3725

Color Glass Condensate

McLerran & Venugopalan hep-ph/9309289

High energy Nuclei/hadrons → large parton density → classical approx.

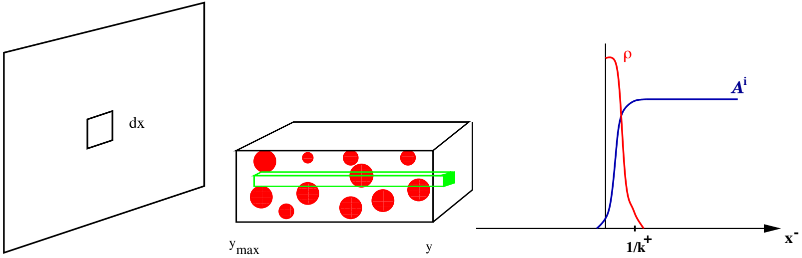

In the limit $1/Q_S << dx << 1$ fm one can neglect

$$| [\mathcal{Q}^a, \mathcal{Q}^b] | = | if^{abc} \mathcal{Q}^c | \ll \mathcal{Q}^2$$

Random distribution of classical color charge.

Color Glass Condensate

- Color: QCD (gluons carry color charge)
- Glass: Stochastic interactions, dynamics on very long time scales (time dilation).
- Condensate: Fields with large occupation # $\sim 1/\alpha_S$ with mom. peaked at $k_T \approx Q_S$

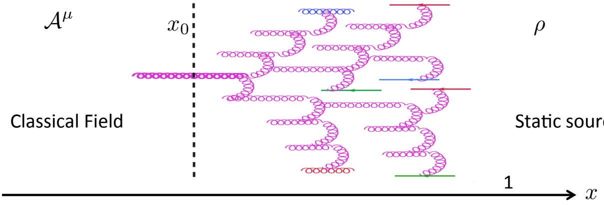

figure :Albacete

A weak coupling effective theory with

- Fast (large-x) partons $\rightarrow$ static classical color source ρ
- Slow (small-x) partons $\rightarrow$ classical gluon fields $\mathcal{A}^\mu$.

McLerran , Venugopalan 1994 (hep-ph/9309289)

Color Glass Condensate

Quantum evolution of the color sources

- given by Renormalization Group description (BK/ JIMWLK).

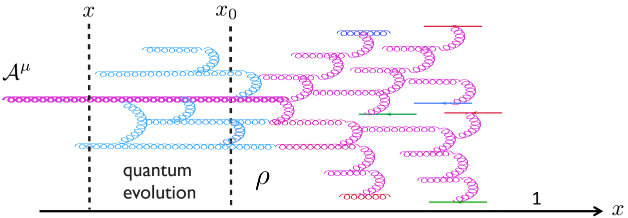

figure :Albacete

$x_0 \to x$ Integrating out degrees of freedom between x and x_0.

Color Glass Condensate:

The Renormalization picture is evident in data.

Limiting fragmentation in $A+A$ and $p+p$.

Busza NPA 854(2011) 57-63

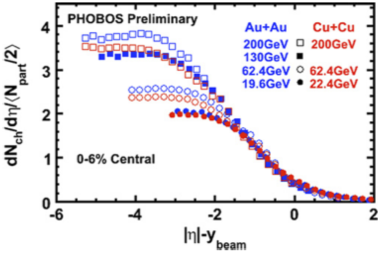

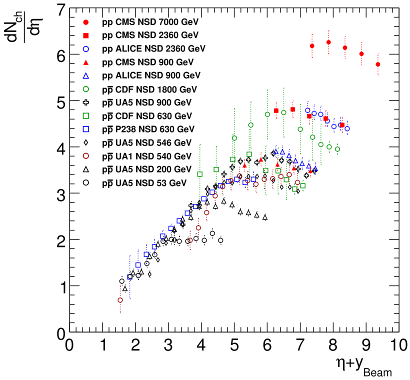

$x \sim e^{\pm y}/\sqrt{s} \Rightarrow$

- Large rapidities d.o.f $\rightarrow$ independent of energy.
- new physics $\rightarrow$ additional d.o.f at small rapidity.

Color Glass Condensate: McLerran-Venugopalan model

- Solve classical Yang-Mills equations

$$[D_\mu, F^{\mu\nu}] = J^\nu$$

for color current due to colliding sources (ρ_1 and ρ_2)

$$J_a^\nu = g\delta^{\nu+}\delta(x^-)\rho_{1,a}(\mathbf{x}_\perp) + g\delta^{\nu-}\delta(x^+)\rho_{2,a}(\mathbf{x}_\perp)$$

- Extract the gauge field after collision for given color charge configuration.

- Final observables $\mathcal{O}(\rho_1, \rho_2)$ should be averaged over color charge configuration

$$\langle\mathcal{O}\rangle = \int [\mathrm{d}\rho_1][\mathrm{d}\rho_2] W_y[\rho_1] W_y[\rho_2] \mathcal{O}(\rho_1, \rho_2).$$

Color Glass Condensate: McLerran-Venugopalan model

Averaging $\langle \mathcal{O} \rangle \Rightarrow$ connection between sources $\Rightarrow$ color correlation.
In the MV model

$$W[\rho] \equiv \exp\left(- \int d^2\mathbf{x}_\perp \frac{\rho^a(\mathbf{x}_\perp)\rho^a(\mathbf{x}_\perp)}{2\,\mu_A^2} \right)$$

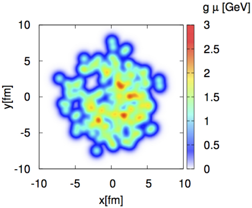

$\rho^a \rightarrow$ random sources distributed from local Gaussian.

fields $\mathcal{A}(\mathbf{x}_\perp) \sim -\rho(\mathbf{x}_\perp)/\nabla_\perp^2 \implies \mathcal{A}(\mathbf{k}_\perp) \sim -\rho(\mathbf{k}_\perp)/\mathbf{k}_\perp{}^2$

Yang-Mills introduces non-local correlation over length scale $1/Q_s$
$\rightarrow$ Glasma flux tube picture.

Gauge fileds after collisions :

- Analytical calculation possible for lowest order of sources. For dilute-dilute(p+p) or dilute-dense(p+A) $\rightarrow$ k_T- factorization.
- For dense-dense (A+A) systems $\rightarrow$ numerical solution on lattice.

IP-Glasma : Classical Yang-Mills approach on 2+1D lattice

Schenke, Tribedy, Venugopalan PRL 108(2012)

E-by-E solve CYM for two colliding nuclei

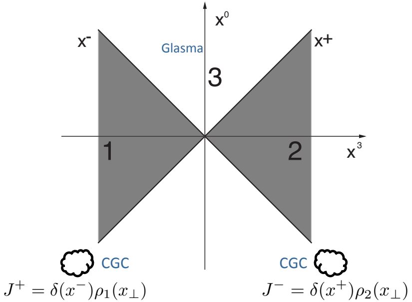

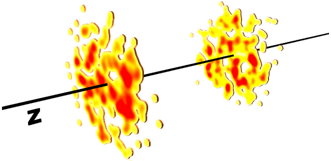

Color charge density for one A+A collision

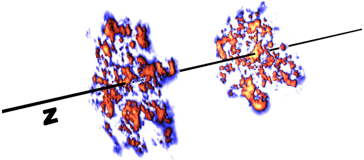

Two point correlator for one A+A collision

$\rho(\mathbf{x}_\perp)$ sampled from local Gaussian distribution $W[\rho]$

$$\left\langle \rho^a(\mathbf{x}_\perp)\rho^b(\mathbf{y}_\perp)\right\rangle = \delta^{ab}\delta^2(\mathbf{x}_\perp - \mathbf{y}_\perp)g^2\mu^2(\mathbf{x}_\perp)$$

lattice implementation Krasnitz, Venugopalan, hep-ph/9809433 Lappi, hep-ph/0303076

IP-Glasma : CYM evolution after collision

Kovner, McLerran, Weigert

The field after collision at $\tau = 0$ has simple relation

$$A^i = A^i_{(A)} + A^i_{(B)} \;,\; A^\eta = \frac{ig}{2}\left[A^i_{(A)}, A^i_{(B)}\right]$$

The fields are evolved at $\tau > 0$ according to

$$[D_\mu, F^{\mu\nu}] = 0$$

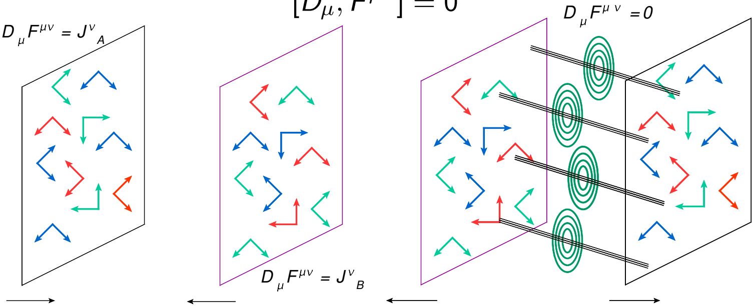

Schenke, Tribedy, Venugopalan PRC 86(2012)

p+A collision at RHIC/LHC

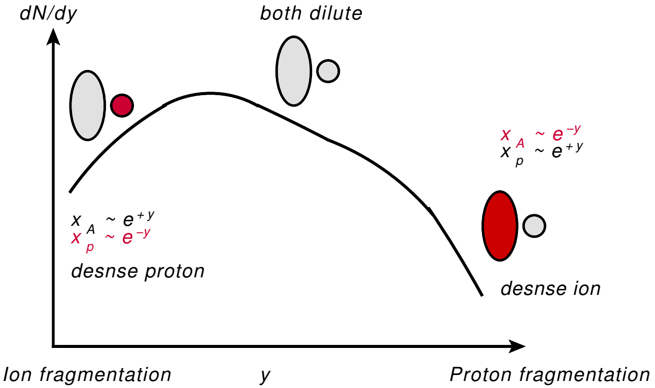

di-hadron correlation in d+A

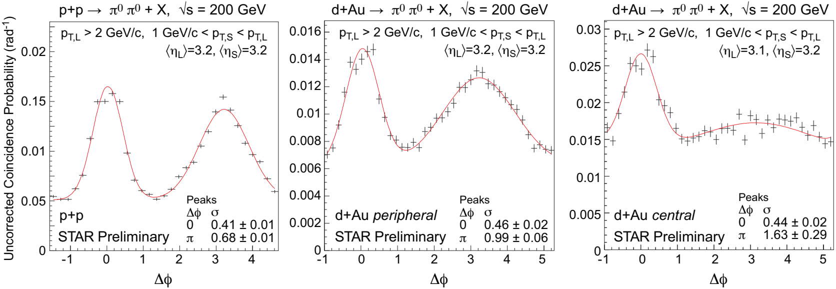

Di-hadron correlations measured at forward rapidities at RHIC:

Suppression factor in d+A/p+A collisions

Quantum correction to gluon production (BK evolutions) predicts strong suppression at higher energy and larger rapidities.

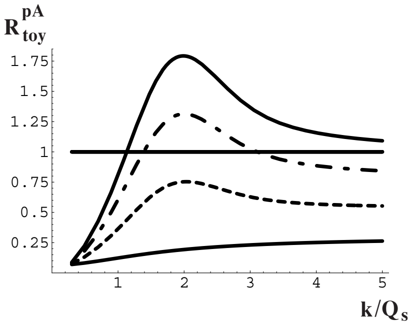

Kharzeev, Kovchegov, Tuchin '03
Kharzeev, Levin, McLerran '02, Albacete '03

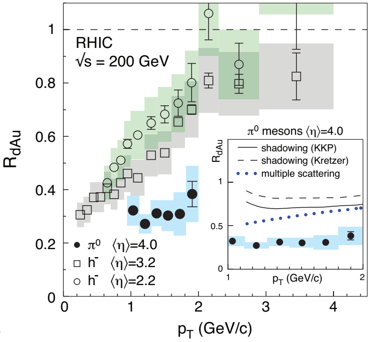

STAR nucl-ex/0602011

No other theory predicts this → confirmed at RHIC.

Suppression factor in d+A/p+A collisions

R_{pA} predictions confirmed by ALICE

Tribedy, Venugopalan 1112.2445

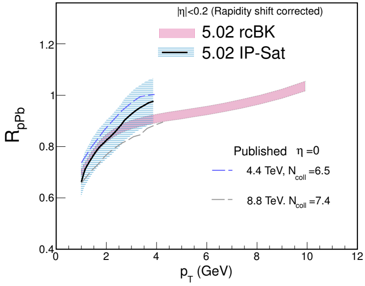

ALICE collab, 1210.4520

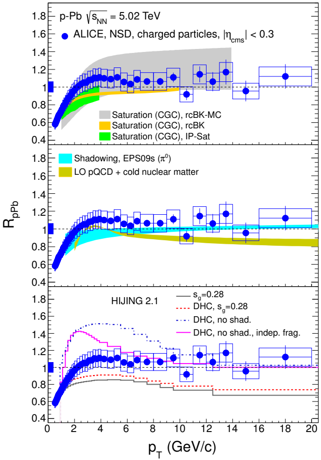

$R_{pPb} \sim 1$ for $p_T \geq 2$ GeV, Growth of proton size (Gribov diffusion) important.

Quark-Pair production in CGC framework

Contributions will come from

Fujii, Gelis, Venugopalan

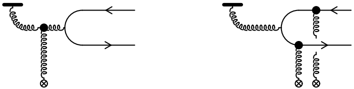

$\otimes \rightarrow$ classical field insertion from dense target.

k_T-factorization not possible and involves higher point correlators $\langle \tilde{U}\tilde{U}^\dagger \tilde{U}\tilde{U}^\dagger \rangle$
$\rightarrow$ can be related to $S(\mathbf{x}_\perp, \mathbf{X}_\perp)$ & un-integrated gluon distribution.

Fujii & Watanabe

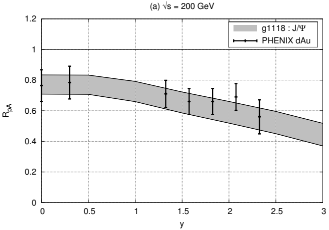

Arnaldi INFN '2013

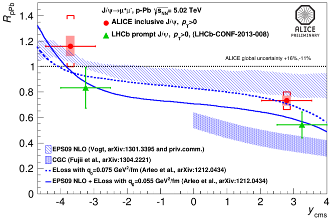

More supression in proton fragmentation region.

Growth of proton size (b), e-by-e fluctuations effects can also be included.

Multiparticle production & sub-nucleonic fluctuations.

Dumitru, Gelis, McLerran, Venugopalan 0804.3858

Correlated multi particle production from disconnected diagrams connected by color averaging.

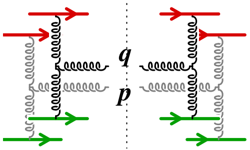

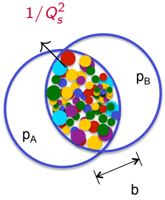

Yang-Mills introduces non-local gauge-field correlation over length scale $1/Q_s \rightarrow$ Glasma flux tube picture.

Two-particle correlation $\rightarrow$ ridge phenomenon.
n-particle correlation $\rightarrow$ Negative-binomial fluctuation.

Gelis, Lappi, McLerran 0905.3234

Ridge phenomenon in p+p and p+Pb

Dusling and Venugopalan

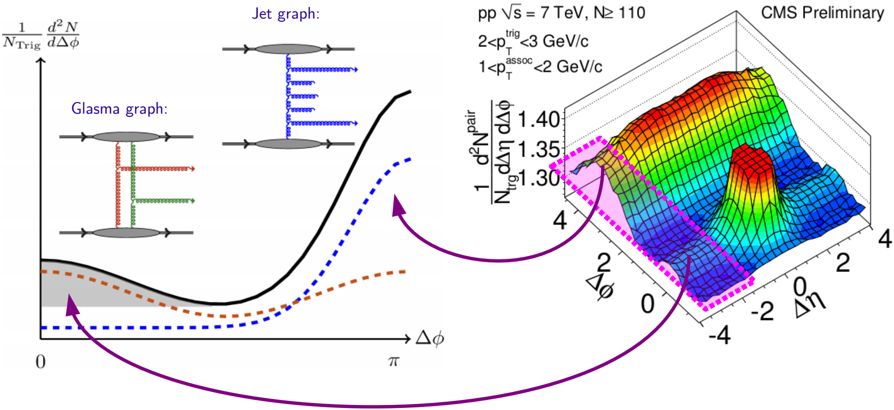

Origin of ridge → quantum interference.

A preferable momentum in hadron w. f. is essential for collimation.

Negative binomial fluctuation

Sources of multiplicity fluctuations are:

- Initial color charge fluctuation at sub-nucleonic length scale $1/Q_S$.
- E-by-E fluctuation of nucleon position and impact parameter.

$\rightarrow$ IP-Glasma generates negative-binomial transverse energy and multiplicity fluctuation Non-perturbatively.

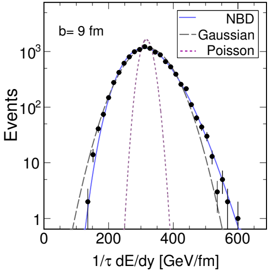

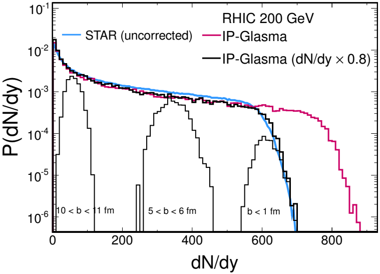

Limiting case of NBD $\rightarrow$ Bose-Einstein (BE) distribution.

Single color gluon emitted from single flux tube $\rightarrow$ BE distribution.
Many sources of color $\rightarrow$ entropy maximisation.

Schenke, PT, Venugopalan PRC 86(2012)

Multiplicity fluctuation in proton+nucleus collisions

Signatures yet to be tested:

Centrality distribution with number of participants of collisions → saturates at large N_{part}, logarithmic increase.

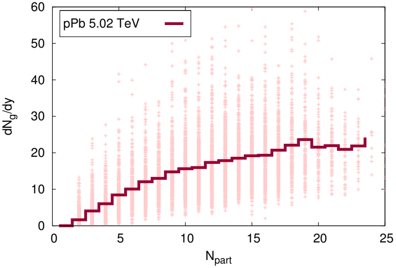

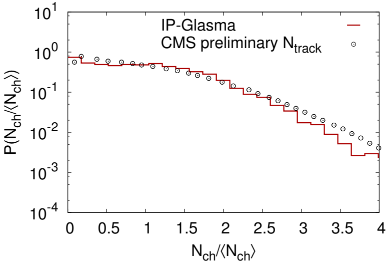

Very different centrality dependence from Wounded nucleon model

Bzdak, Skokov 1307.6168

Initial geometry in p+p and p+A/d+A collisions

System size (very similar) and initial eccentricities (very different) for same multiplicity.

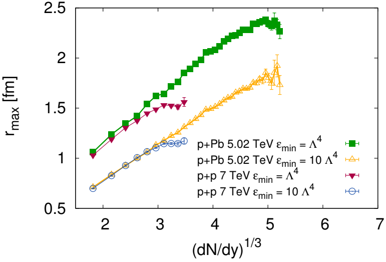

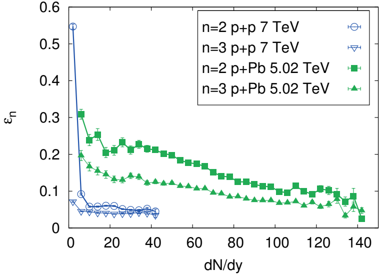

$r_{max} \rightarrow$ maximal radius with $\varepsilon_{\rm min} \sim \Lambda^4_{\rm QCD}$

$r_{max} \propto (dN/dy)^{1/3}$, comparable HBT radii in p+p and p+Pb.

p+p $\rightarrow \epsilon_{2,3}$ are significantly smaller and flat with multiplicity.

Smaller eccentricities for high multiplicity events.

Initial geometry and fluctuations in A+A

IP-Glasma provides good description of initial geometry and fluctuations in Pb+Pb and Au+Au.

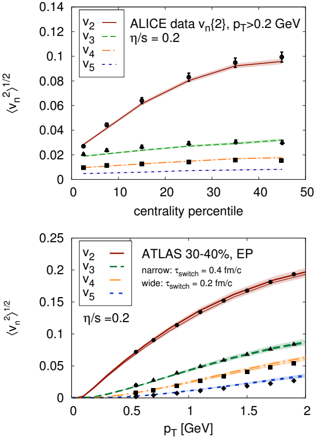

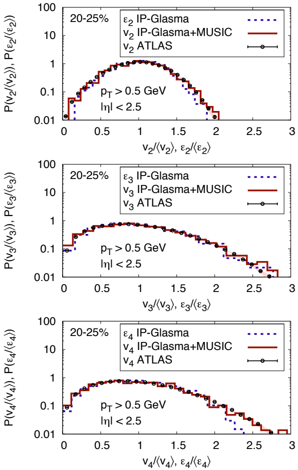

A combined Yang-Mill + viscous hydro calculation for the first time describes all measured harmonics and its e-by-e fluctuations.

Energy density (ϵ) from IP-Glasma model (at $\tau = 0$)

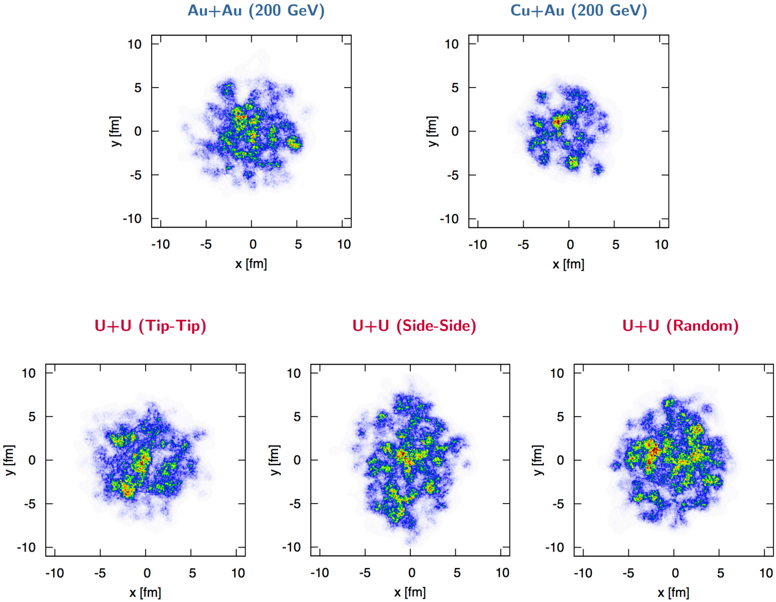

Centrality dependence in A+A at LHC

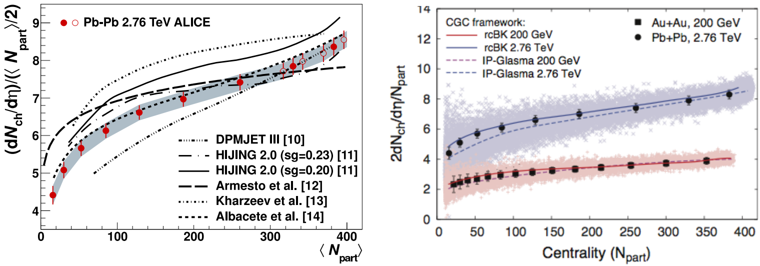

ALICE 1012.1657

CGC centrality dependence of $A + A \to$ consistent with ALICE.

Centrality dependence in A+A at RHIC

- Local Running coupling on each point on lattice $\alpha_s\left(Q_s^{max}(\mathbf{x}_\perp)\right)$

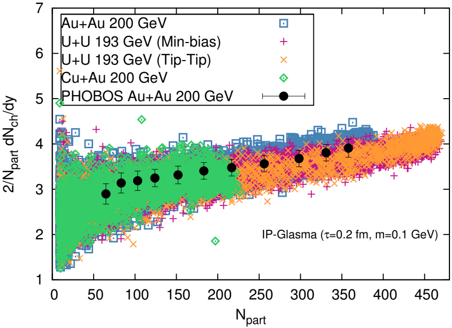

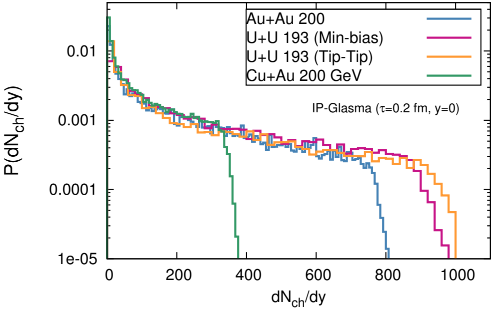

Larger systems → smaller multiplicity per participants.
U+U min-bias & tip-tip are very close unlike 2-component model.

$\frac{dN_{ch}}{dy} \sim \frac{Q_s^2 S_\perp}{\alpha_S(Q_s^{max})}$, for Tip-Tip U+U, $Q_s^2 \uparrow$ but $S_\perp \downarrow$

Eccentricity for different systems

The spatial eccentricities that characterize the geometry

$$\varepsilon_n = \frac{\sqrt{\langle r^n \cos(n\phi)\rangle^2 + \langle r^n \sin(n\phi)\rangle^2}}{\langle r^n \rangle}, \ \langle\cdots\rangle \to \text{weight}\, \epsilon(\mathbf{x}_\perp, \tau)$$

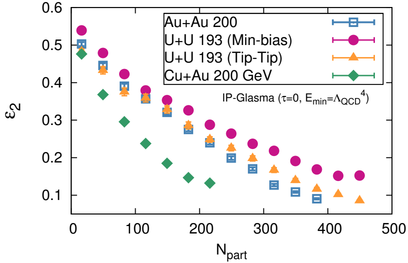

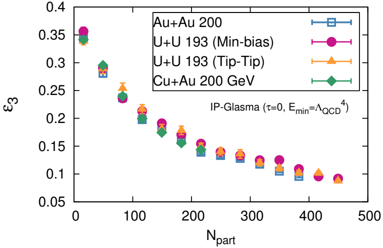

- ε_2 very sensitive to initial geometry of colliding system.
- Fluctuation driven moment ε_3 are very similar for different systems.

Summary

- CGC is an universal descrip1on of high energy saturated hadron/nucleus, an *ab inito* (first principle) approach.
- Powerful framework for wide range of system e+p, e+A, p+p, p+A, A+A.
- Phenomenologically successful in describing bulk features of data, difficult in conventional pQCD approach.
- Multi particle production can be studied in detail, consistently describes global data over wide range of energies/systems.
- Framework includes different sources of quantum fluctuations, successful describe the initial dynamics of heavy ion collisions.

BACK UP SLIDES

Higher order moments ϵ_3, ϵ_5

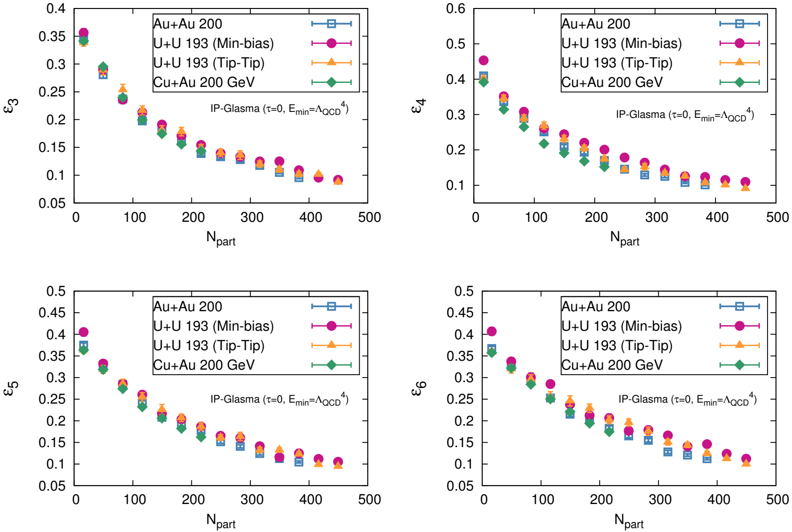

Fluctuation driven moments are very similar for different systems.

Flow in p+A collisions.

A strong dependence on choice of initial conditions for large N_{part}.

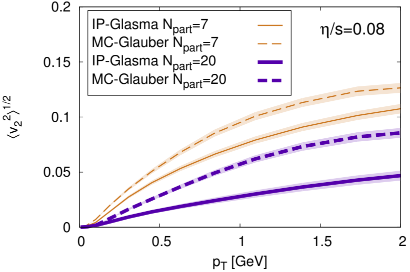

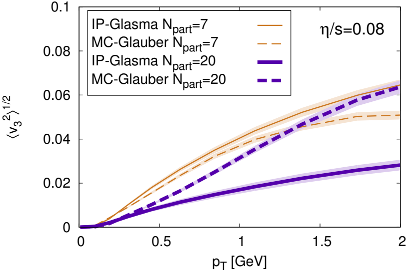

Both v_2 and v_3 are smaller in IP-Glasma compared to MC-Glauber.

Flow in d+A collisions at RHIC.

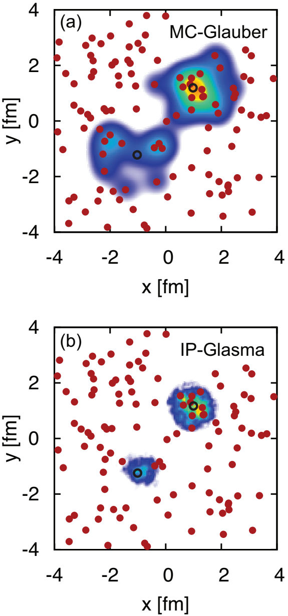

Deuteron nucleus sampled from,

$$\phi_{\rm pn}(r) = \frac{1}{\sqrt{2\pi}} \frac{\sqrt{ab(a+b)}}{b-a} \frac{e^{-ar} - e^{-br}}{r}$$

$\langle r \rangle \sim 2.52$ fm $\rightarrow$ separated regions

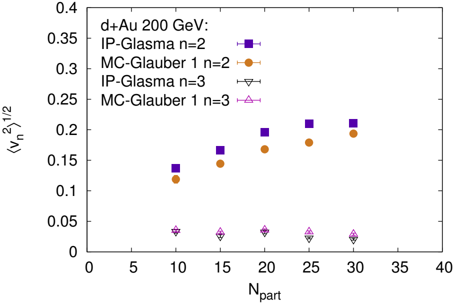

ϵ_n will influence v_n only for small r

Viscous correction in smaller sized systems

Relative magnitude of the ideal and the viscous terms are compared over the evolution time $T^{\mu\nu} = T_0^{\mu\nu} + \pi^{\mu\nu}$
Switch IP-Glasma $\leftrightarrow$ Hydro $\tau = 0.2$ fm, $\frac{\eta}{s} = 0.2$ (fits to Pb+Pb data),

25 % viscous correction:

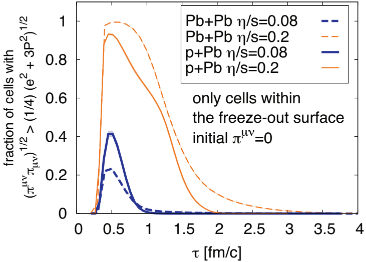

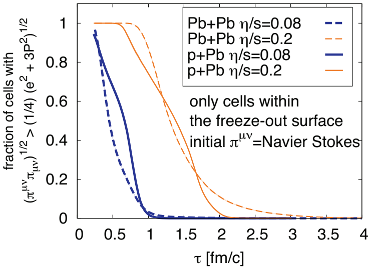

Navier-Stokes initialization $\pi_0^{\mu\nu} = \eta\left(\nabla^\mu u^\nu + \nabla^\nu u^\mu - \frac{2}{3}\Delta^{\mu\nu}\nabla_\lambda u^\lambda\right)$

Large correction $(\sqrt{\pi_{\mu\nu}\pi^{\mu\nu}}/\sqrt{e^2 + 3P^2})$ over significant fraction of life time.

Viscous correction in smaller sized systems

Life time of p+Pb $\sim \frac{1}{6}$ life time of Pb+Pb.

50 % viscous correction:

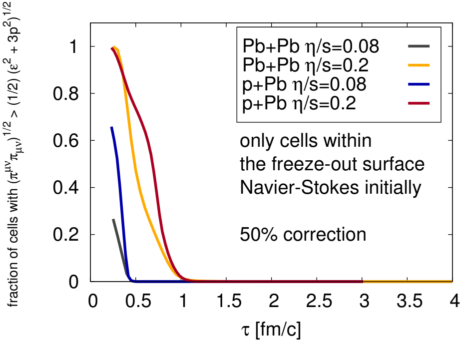

Might question reliability of second order viscous hydrodynamics for smaller systems.

IP-Glasma : Multiplicity and Energy density

E-by-E soln. of CYM equation on 2+1D lattice $\rightarrow F^{\mu\nu}(\tau, \mathbf{x}_\perp, \eta)$.

- Multiplicity (n): $F^{\mu\nu}(\tau, \mathbf{x}_\perp, \eta) \rightarrow \mathcal{H}(\mathbf{x}_\perp)$ (Hamiltonian density)
  Fourier transform $\mathcal{H}(\mathbf{k}_\perp) \rightarrow$ number density $n(\mathbf{k}_\perp)$ of gluon,
  $\mathcal{H}(\mathbf{k}_\perp) \sim n(\mathbf{k}_\perp)\omega(\mathbf{k}_\perp)$, assuming dispersion relation, $\omega(k) = k$

  In the transverse Coulomb Gauge :

$$\frac{dN_g}{dy} = \frac{2}{N^2}\int \frac{d^2k_T}{\tilde{k}_T}\left[\frac{g^2}{\tau}\mathrm{tr}\left(E_i(\mathbf{k}_\perp)E_i(-\mathbf{k}_\perp)\right) + \tau\,\mathrm{tr}\left(\pi(\mathbf{k}_\perp)\pi(-\mathbf{k}_\perp)\right)\right]$$

- Energy density (ϵ): $F^{\mu\nu} \rightarrow T^{\mu\nu}$ (stress energy tensor).

$$T^{\mu\nu} = -g^{\gamma\delta}F^{\mu}_{\ \gamma}F^{\nu}_{\ \delta} + \frac{1}{4}g^{\mu\nu}F^{\gamma}_{\ \beta}F_{\gamma}^{\ \delta}$$

  solving eigen value eq. $u_\mu T^{\mu\nu} = \epsilon u^\nu$ gives ϵ and flow u^ν
  $T^{\mu\nu}_{CYM}$ can be Landau matched with viscous hydro.

Gale, Jeon, Schenke, Tribedy, Venugopalan 1209.6330

p+p, p+A and A+A eccentricities

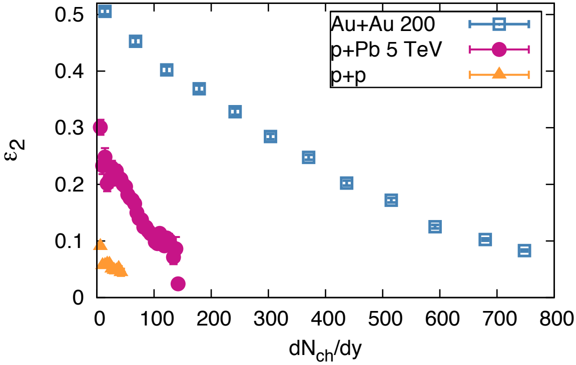

Flow in d+A collisions at RHIC.

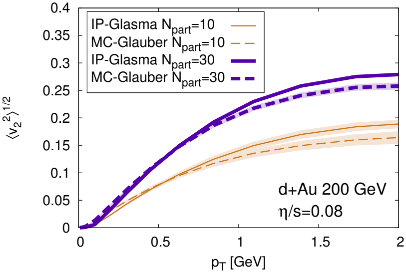

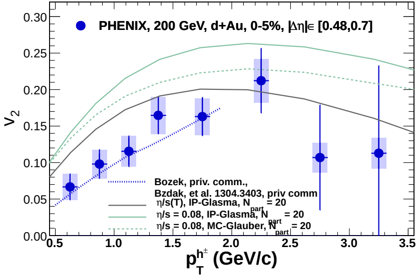

Different models of initial conditions.

I.C.	Geometry	$k_T - factorization$	Classical Yang-Mills
framework	2-component model	CGC perturbative	CGC non-perturbative
E-by-E	✓	✓	✓
Sub-nucleonic fluctuation	✗	✗	✓
Time evolution	✗	✗	✓
Initial flow	✗	✗	✓
NBD fluctuation	by hand	by hand	✓

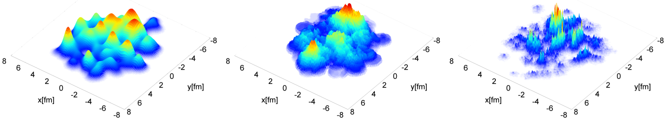

Comparison with MC-Glauber model

Bzdak, Schenke, PT, Venugopalan

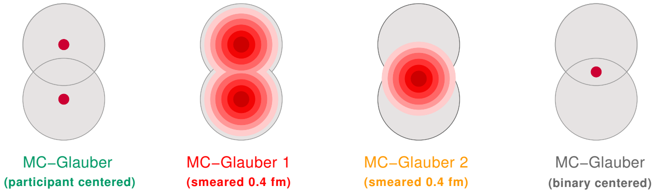

MC-Glauber $\rightarrow$ smearing width σ_0 $\rightarrow$ free parameter.

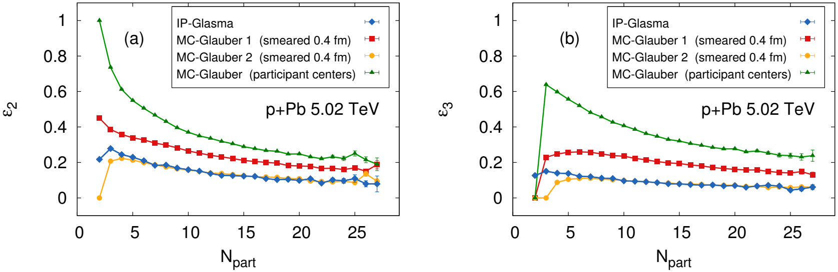

Very different behaviour at small N_{part}, would effect v_n/ϵ_n computation.

Binary centered $\leftrightarrow$ IP-Glasma, no energy deposition due to pure gauge fields outside overlap.

Flow in p+p and p+A collisions.

Viscous hydrodynamic simulation using MUSIC with IP-Glasma & MC-Glauber 1 (participant centred, smeared 0.4 fm)

$\frac{\eta}{s} = \frac{1}{4\pi}, \tau_0 = 0.2fm$ and $T_{f0} = 120$ MeV.

Integrated $\langle v_n \rangle$ for $p_T > 0.5GeV$.

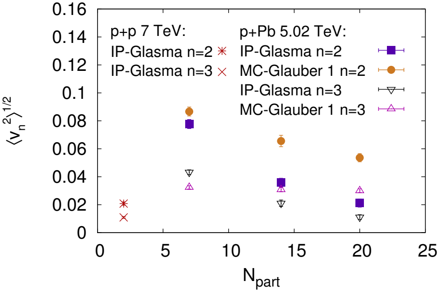

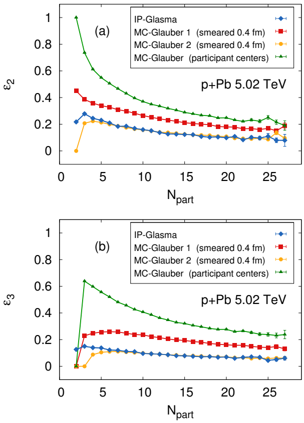

Flow in p+p and p+Pb at large N_{part} are similar for IP-Glasma.

N_{part} dependence of $v_2 \rightarrow$ high sensitivity on initial conditions.